Ground-state and excitation spectra of the negative-U Hubbard model

H. E. Castillo* and C. A. Balseiro
Centro Atómico Bariloche and Instituto Balseiro, 8400 San Carlos de Bariloche, Argentina
(Received 26 September 1991)

We study the negative-U Hubbard model by exact diagonalization of a 4×4 cluster with different numbers of particles. We calculate the ground-state energy and wave function as well as the one-particle, charge-, and spin-excitation spectra. We show that the BCS approximation gives results in good agreement with the exact ones for the ground-state energy and wave function in the whole range of U. In the one-particle excitation spectrum the BCS dispersion relation gives the position of the most intense peaks of the exact calculation. Lower-energy (quasiparticle) excitations, which are interpreted as strongly dressed Bogoliubov quasiparticles, also appear. The occurrence of pair-breaking and collective excitations in the charge- and spin-excitation spectra and the interplay between one-particle and collective modes are discussed.

I. INTRODUCTION

The discovery of high-temperature superconducting materials has opened questions in the fields of superconductivity and strongly correlated systems, but has also renewed the interest in some old unanswered ones. The short coherence length of these superconductors suggest that they are probably in an intermediate regime between BCS weak-coupling superconductivity and Bose condensation of composite bosons. This has triggered efforts toward the understanding of the evolution between these two regimes.[1–3] A simple model which can be used to describe this evolution is the negative-U Hubbard model. This model, however, does not include long-range interactions, and consequently collective excitations that involve charge redistribution which should have energies of the order of the plasma frequency occur at low energies. If experimental data are interpreted in terms of this type of model, one should bear in mind this unphysical feature.

It has been shown that the BCS wave function evolves continuously as the interaction strength changes and that it is a good variational ansatz both in the weak- and in the strong-coupling limits.[4,5] The slave-boson technique has also been used to study the ground state, showing only a slight improvement in the energy for intermediate values of the interaction strength.[6] However, the excitations are quite different in both limits: pair-breaking excitations with an energy gap 2Δ dominate in weak coupling, while in strong coupling strongly bound states exist and the lowest-energy excitations are collective modes like those of superfluid He, pair-breaking excitations being much higher in energy.[5,3]

In this work we study the ground-state and excitation spectra of the two-dimensional (2D) negative-U Hubbard model with exact diagonalization techniques[7] in a finite cluster, for the whole range of interaction strengths. We examine the validity of the mean-field approximation for the ground-state energy and wave function, and study charge, spin, and one-particle excitations. We show that in the one-particle spectral densities there is a broad and intense maximum at the energy of the BCS quasiparticle, there are also low-energy quasiparticle lines which correspond to a strongly dressed BCS excitation. In the strong-coupling limit this problem has been studied by mapping the Hamiltonian into a polarized t-J model.[8,9]

The rest of the paper is organized as follows: in Sec. II we present the model and numerical method; in Sec. III we present our results for the ground state (III A), for the one-particle (III B), the charge-charge (III C), and the spin-spin (III D) Green's functions, and we study (III E) the coupling between one particle and collective modes; and finally Sec. IV includes a summary and discussion.

II. MODEL AND NUMERICAL METHOD

The negative-U Hubbard model is given by the Hamiltonian:

$$H = -t \sum_{(ij)} (c^{\dagger}_{i\sigma} c_{j\sigma} + \text{H.c.}) - U \sum_{i} n_{i\uparrow} n_{i\downarrow} , \qquad (1)$$

where $c^{\dagger}_{i\sigma}$ creates a particle at site i with spin σ, $n_{i\sigma} = c^{\dagger}_{i\sigma} c_{i\sigma}$ is the number operator for site i with spin σ, t is the hopping matrix element, and U is the strength of the attractive interaction ($U > 0$).

We have diagonalized exactly the Hamiltonian in a finite cluster of 4×4 sites, with periodic boundary conditions and different numbers of particles. The calculations of the ground-state energy and wave functions were performed using a modified Lanczos method.[7] In these calculations the translation and inversion symmetries of the cluster were used, as well as the spin-inversion symmetry.

We also calculated frequency-dependent correlation functions. To study one-particle excitations we calculated the one-particle Green's function $\langle\langle c_{\mathbf{k}\sigma}, c^{\dagger}_{\mathbf{k}\sigma} \rangle\rangle_{\omega}$,

where $c^{\dagger}_{\mathbf{k}\sigma}$ creates an electron with crystal momentum $\mathbf{k}$ and spin σ. The charge and spin excitations were studied by means of the two-particle Green's functions $\langle\langle n_{-\mathbf{q}}, n_{\mathbf{q}}\rangle\rangle_\omega$ and $\langle\langle S^z_{-\mathbf{q}}, S^z_{\mathbf{q}}\rangle\rangle_\omega$, $n_{\mathbf{q}}$ and $S^z_{\mathbf{q}}$ are the Fourier transforms of the charge and z component of the spin densities, respectively.

We obtained results for numbers of electrons $N_e = 2, 4, 6$, and 8. The case of a nearly half-filled band, which in the present case would correspond to $N_e \simeq 16$ may be interesting, since for this filling superconductivity and charge density waves compete.[10,2] Unfortunately, the Hilbert space for a nearly-half-filled band in this cluster is too large for our computing facilities and we were forced to restrict ourselves to lower densities.

III. RESULTS

A. Ground state

First we present results for the ground-state energies for different values of U/t and N_e. All the results presented below correspond to ground states calculated in the sector of zero magnetization, i.e., $N_\uparrow = N_\downarrow$. In Fig. 1 the ground-state energy E_0 as a function of U is shown for $N_e = 4, 6$, and 8 particles. The continuous line is the result obtained in the BCS approximation. The BCS energy was obtained by solving the mean-field equations in the same cluster. In order to compare in a more quantitative way the exact results with mean-field theory we plot in Fig. 2 the relative difference between both energies. The maximum relative difference is obtained for intermediate coupling, U of the order of the one-particle half-bandwidth $W = 4t$, and is always smaller than 3.5%. These results show that the BCS mean-field theory is an excellent approximation for the ground-state energy in the whole range of parameters.

A direct comparison of the exact wave function with the BCS ansatz is not feasible because the latter does not conserve the total number of particles. One possibility is to project the BCS wave function into the subspace with a given number of particles. Another possibility is to calculate expectation values of different observables.

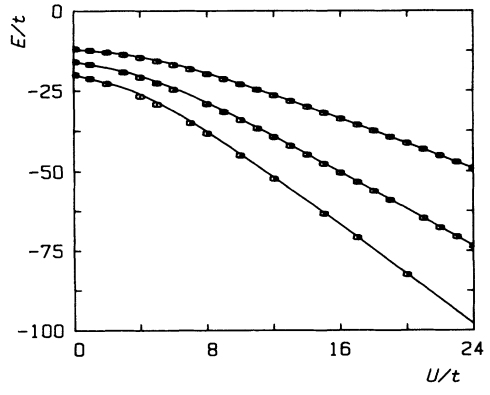

FIG. 1. Ground-state energy as a function of U for $N_e = 4$ (upper curve), 6 (middle curve), and 8 particles (lower curve). Squares: exact results, solid line: BCS approximation with parameters determined self-consistently for the 4 × 4 cluster.

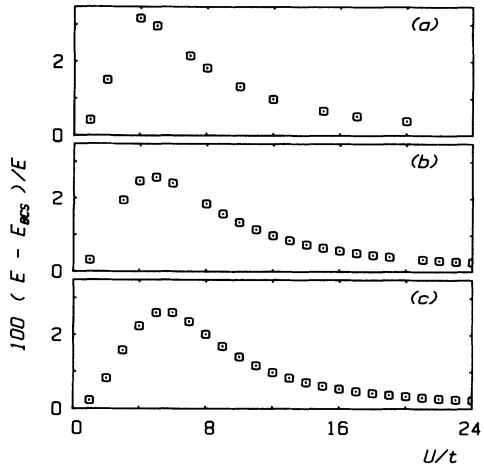

FIG. 2. Relative difference between the exact value and the BCS approximation for the ground-state energy for (a) $N_e = 8$, (b) $N_e = 6$, and (c) $N_e = 4$.

We have used the second approach, in Fig. 3 we show the expectation value of $n_{\mathbf{k}\sigma}$ for different values of U, $N_e = 6$, and all the inequivalent wave vectors $\mathbf{k}$ compatible with the cluster. The continuous lines in the figure are the mean-field results as obtained for the same cluster, for display purposes we considered $\mathbf{k}$ as a continuous variable. Again, we see an excellent agreement between the exact and mean-field results, only for intermediate values of U there is an appreciable difference for the case of $\mathbf{k} = 0$. Similar results were obtained for other particle numbers N_e.

Finally, we calculated the chemical potential μ as a function of U and the particle density $n = N_e/16$. In the thermodynamic limit, the chemical potential is defined as $\mu = \partial E_0/\partial N_e$. We have to calculate μ as the difference between ground-state energies with different numbers of particles. Note that even and odd numbers of particles behave very differently in the large-U limit, where the total energy is essentially given by the number of pairs times $-U$. Consequently we define

$$\mu = \tfrac{1}{2}[E_0(N_e) - E_0(N_e - 2)] \,. \tag{2}$$

In Fig. 4 the chemical potential shifted by the Hartree-Fock correction $\mu^\star = \mu + \frac{1}{2}Un$ as a function of N_e is shown for different values of U. For $N_e = 2$ the chemical potential is half the energy of the two-particle bound state, as the number of particles increases, $\mu^\star$ also increases and, depending on the parameters may get into the one-particle band starting at $-4t$. This means that the chemical potential μ gets into the Hartree-Fock one-particle band, whose bottom is at $-4t-\frac{1}{2}Un$. These results are also in good agreement with mean-field theory.

All the numerical results presented above show that the BCS approximation correctly describes the ground state of the system. It evolves continuously from the small-U to the large-U limits, as was pointed out previously. However, our calculations do not give much information for the weak-coupling system, since the coherence length in this limit is larger than the size of the cluster. The

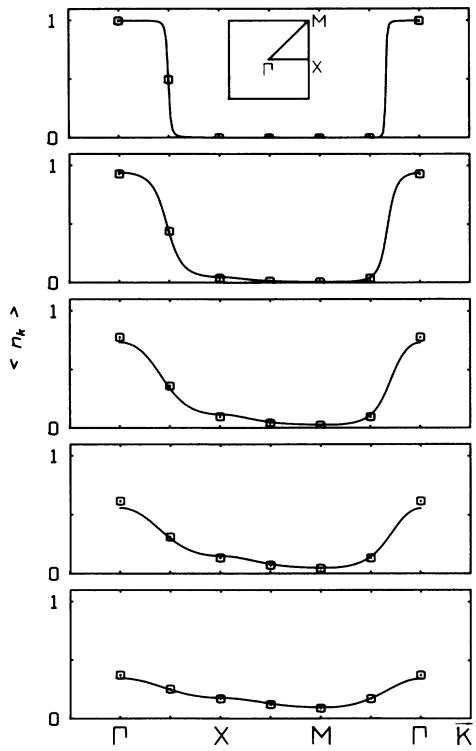

FIG. 3. Expectation values of $n_{\mathbf{k}\sigma}$ for $N_e = 6$, with $U = 1, 4, 7, 10$, and 20 (from upper to lower boxes). Squares: exact results, solid line: BCS approximation with parameters determined self-consistently for the 4×4 cluster. The inset shows the points considered in the first Brillouin zone.

excitations are expected to be very different from the mean-field excitations in the intermediate and large-U limits. In the following sections we show that this is indeed the case.

B. One-particle spectral densities

We calculated the one-particle spectral densities defined as

$$A_\sigma(\mathbf{k},\omega) = -\frac{1}{\pi}\mathrm{Im}\left(\left\langle\Phi_0\left|c_{\mathbf{k}\sigma}\frac{1}{\omega + i0^+ - H + E_0}c^\dagger_{\mathbf{k}\sigma}\right|\Phi_0\right\rangle + \left\langle\Phi_0\left|c^\dagger_{\mathbf{k}\sigma}\frac{1}{-\omega + i0^+ - H + E_0}c_{\mathbf{k}\sigma}\right|\Phi_0\right\rangle\right), \tag{3}$$

where $|\Phi_0\rangle$ and E_0 are the wave function and energy of the ground state, respectively, the first term on the right-hand side of Eq. (3) gives the contribution corresponding to adding a particle to the system and is related with the inverse photoemission experiment, the second term corresponds to removing a particle and gives the photoemission spectrum.

The one-particle density of states is given by

$$D(\omega) = \frac{1}{2N}\sum_{\mathbf{k},\sigma} A_\sigma(\mathbf{k},\omega)\,. \tag{4}$$

In Fig. 5 the one-particle density of states is shown for $N_e = 4$ and different values of U. As is clearly seen, there is a gap at the Fermi energy which increases as U increases. In Fig. 6 the size of the gap is compared

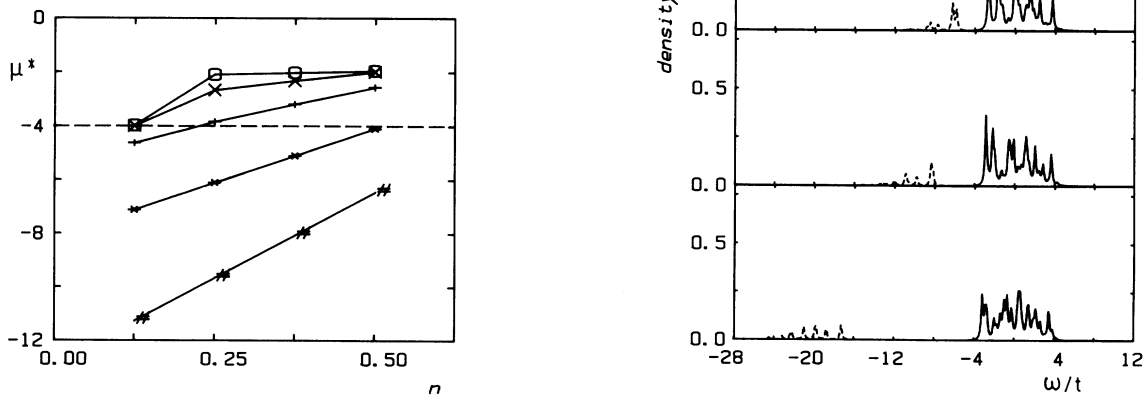

FIG. 4. Chemical potential shifted by the the Hartree-Fock correction $\mu^\star = \mu + \frac{1}{2}Un$ as a function of the density; for (□) $U = 1$, (×) $U = 4$, (+) $U = 8$, (*) $U = 15$, and (#) $U = 25$. The dashed line is at the bottom of the one-particle band. The solid lines are only to guide the eye.

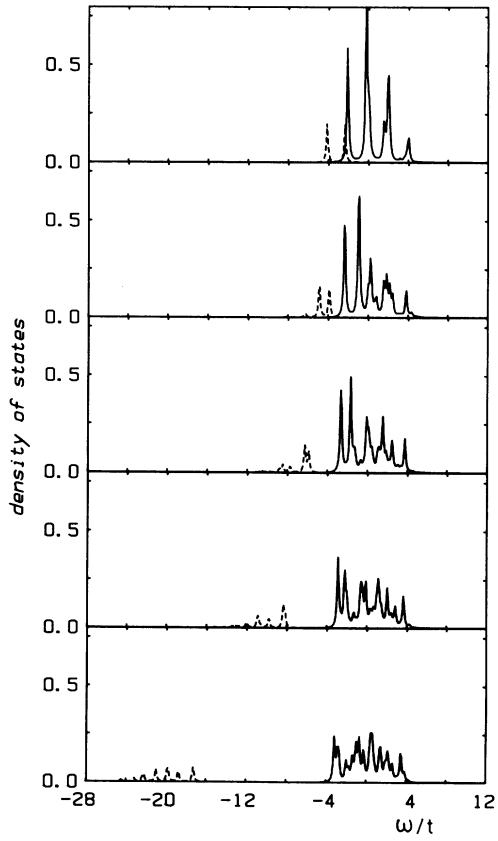

FIG. 5. One-particle density of states for $N_e = 4$, with $U = 1, 4, 7, 10$, and 20 (from upper to lower boxes). Dashed line: density of occupied states; solid line: density of empty states. The delta functions have been broadened by including a small imaginary part $\eta = 0.1t$.

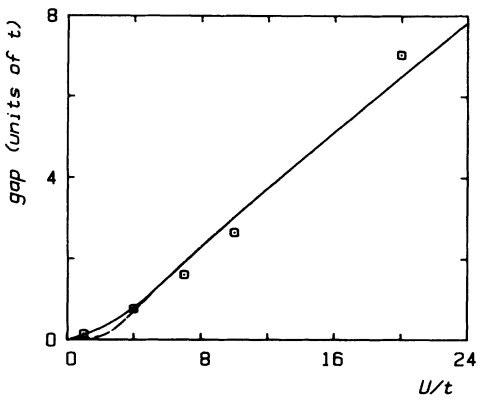

FIG. 6. One-particle gap as a function of U for $N_e = 4$. Squares: exact results obtained from one-particle Green's functions, solid line: BCS gap parameter for the same cluster, dashed line: BCS gap parameter for a 16×16 system with the same density. Finite-size effects appear only for small U.

with the results of the BCS approximation. The same behavior is observed for other particle numbers, and the gap is always pinned to the Fermi energy. Similar results were obtained by Dagotto *et al.* in a $\sqrt{10} \times \sqrt{10}$ cluster.[11]

It is instructive to analyze the behavior of the one-particle spectral densities $A_\sigma(\mathbf{k},\omega)$ for different values of $\mathbf{k}$. In Fig. 7 the spectral densities are depicted for all the nonequivalent $\mathbf{k}$'s of the lattice. Each peak in the spectral density is indicated by a horizontal line with a length proportional to the amplitude of the peak. The dispersion relation of the BCS quasiparticles $E_\mathbf{k}$ is shown with a continuous line, the parameters used to calculate this line are the self-consistent solutions of the mean-field equations for the same cluster and the same U and N_e of the exact calculation. It can be seen that the mean-field dispersion relation almost fits—without any free parameter—the most intense peaks of the exact calculation. These peaks may be associated with the undressed BCS quasiparticle. The amplitude of photoemission peaks is small except for $\mathbf{k}$ close to the Γ point due to the coherence factor $v_\mathbf{k}$. In the inverse photoemission spectra all peaks but the ones corresponding to the zone center are intense as suggested by the mean-field calculation, which predicts an amplitude given by $u_\mathbf{k}^2$. These strong peaks are surrounded by lower intensity ones which, in the thermodynamic limit, presumably form a continuum giving rise to a resonance with a finite width, reflecting the fact that the BCS Bogoliubov quasiparticles acquire a finite lifetime. For most values of $\mathbf{k}$ these are not the lowest energy one-particle excitations; there are peaks of small intensity much closer to the Fermi energy than $E_\mathbf{k}$. In what follows we refer to these peaks as the quasiparticle peaks and as we show below they correspond to strongly dressed Bogoliubov quasiparticles.

C. Charge excitations

In this and the next section we discuss the nature of collective excitations of the system with a given number of particles. These are charge and spin excitations, which will dominate the thermodynamics of the system. The charge excitations are studied by means of the frequency-dependent density-density correlation function, given by

$$\Pi(\mathbf{q},\omega) = \left\langle \Phi_0 \left| n_{-\mathbf{q}} \frac{1}{\omega + i0^+ - H + E_0} n_\mathbf{q} \right| \Phi_0 \right\rangle , \qquad (5)$$

where $n_\mathbf{q}$ is the Fourier transform of the particle density. Note that this is not the complete Green's function usually associated with the polarization, normally given by Eq. (5) antisymmetrized.

In the large-U limit we expect two kinds of excitations in different energy ranges to contribute to $\Pi(\mathbf{q},\omega)$: on one hand pair-breaking excitations at energies larger than 2Δ and on the other hand collective excitations of the hard-core Bose gas at low energies. This collective mode has been studied in the large-U limit using a canonical transformation of the original Hamiltonian,[12,13] and for arbitrary U with a RPA approximation.[3]

The total density of charge excitations, $(1/N)\sum_\mathbf{q} -(1/\pi)\mathrm{Im}\Pi(\mathbf{q},\omega)$ is shown in Fig. 8. In the intermediate-

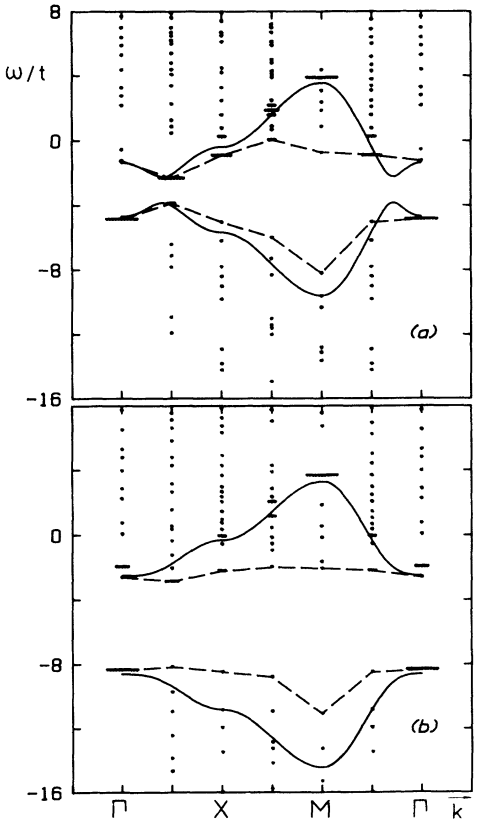

FIG. 7. One-particle spectral densities for $N_e = 4$ and all values of $\mathbf{k}$, with (a) $U = 4$ and (b) $U = 10$. Each peak in the spectral density is indicated by a horizontal line with a length proportional to the amplitude of the peak. Solid line: dispersion relation of the unperturbed BCS quasiparticle $E_\mathbf{k}$ calculated with self-consistent parameters corresponding to the same cluster. The dashed line is only a guide to the eye and joins the exact energies of quasiparticle peaks for different $\mathbf{k}$ values.

U case, the separation between the low-energy excitations and the high-energy excitations is clearly observed. The former are the collective excitations while the latter correspond to pair-breaking excitations which contribute with a small weight to Π. As U decreases the characteristic energy of both types of excitations become of the same order and for small U we cannot distinguish one from the other. For large U the weight of pair-breaking excitations is so small that they are hardly observed.

In Fig. 9 we show the spectral density of charge excitations defined as $-(1/\pi)\mathrm{Im}\Pi(\mathbf{q},\omega)$, for all values of $\mathbf{q}$ and different values of U. The plot is done as in Fig. 7. For each value of $\mathbf{q}$ the peak with larger amplitude is the lowest energy peak, it corresponds to a collective state. The dispersion relation of this state is indicated with a dashed line in the figure. Although this dispersion relation is affected by finite-size effects, there are some general features which are well described by the calculations. For $\mathbf{q} = 0$ the corresponding energy is zero. This reflects a symmetry of the system associated with particle conservation. In the thermodynamic limit this symmetry gives rise to a Goldstone mode with a dispersion relation linear in q. For $\mathbf{q} = (\pi/a, \pi/a)$ the energy of the collective mode is $-U-2\mu$. This has been shown by Zhang[14] who defined

$$J_+ = \sum_j e^{i\mathbf{Q}\cdot\mathbf{R}_j} c_{j\uparrow}^\dagger c_{j\downarrow}^\dagger \tag{6}$$

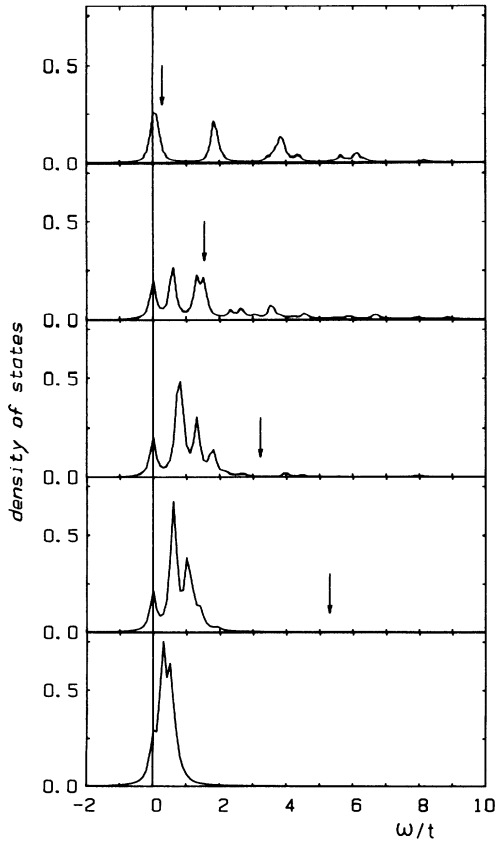

FIG. 8. Total density of charge excitations for $N_e = 4$, with $U = 1, 4, 7, 10$, and 20 (from upper to lower boxes); and $\eta = 0.1t$. The arrows show the position of 2Δ for each value of U.

with $\mathbf{Q}$ the wave vector at the zone corner and $\mathbf{R}_j$ the coordinate of site j. It can be easily shown that J_+ is an operator satisfying the equation

$$[H, J_+] = (-U - 2\mu)J_+ , \tag{7}$$

thus J_+ acting on the ground state creates an exact eigenstate of H with energy $E_0 - U - 2\mu$. If we use the chemical potential μ as defined in Eq. (2) we find that the energy of the peak corresponds exactly to this value.

In Fig. 9(b) it becomes more evident that there are two energy scales: pair-breaking excitations with energy greater or equal than 2Δ and collective excitations with a much smaller energy.

As a general trend we see that the bandwidth associated with the collective excitation decreases as U increases. As was shown previously[3] an RPA calculation for this mode is in qualitative agreement with the numerical results.

D. Spin excitations

To study spin excitations we calculated the frequency dependent spin-spin correlation function, given by

$$\chi(\mathbf{q},\omega) = \left\langle \Phi_0 \left| S_{-\mathbf{q}}^z \frac{1}{\omega + i0^+ - H + E_0} S_{\mathbf{q}}^z \right| \Phi_0 \right\rangle , \tag{8}$$

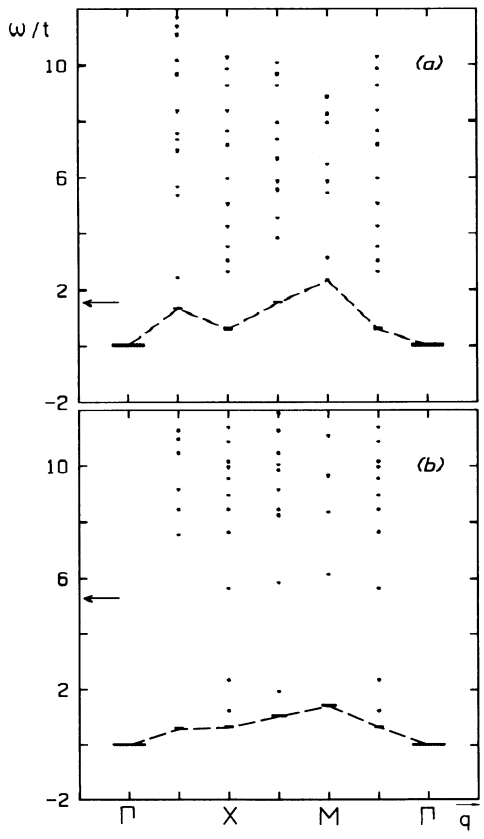

FIG. 9. Spectral densities of charge excitations for $N_e = 4$ and all values of $\mathbf{q}$ with (a) $U = 4$ and (b) $U = 10$. The plot is done as in Fig. 7. The arrows show the position of 2Δ for each value of U. The dashed lines are guides to the eye and join the lowest charge excitation energies.

where $S^z_{\mathbf{q}}$ is the Fourier transform of the z component of the spin of the particle. As before, this is not the complete Green's function usually associated with the susceptibility.

The total density of spin excitations, defined as $(1/N)\sum_{\mathbf{q}} -(1/\pi)\mathrm{Im}\chi(\mathbf{q},\omega)$ is shown in Fig. 10. The integral I of this density decreases as U increases. This is due to a sum rule that yields $I = (1/N)\sum_i < (S^z_i)^2 >= n/4 - (1/2N)\sum_i < n_{i\uparrow} n_{i\downarrow} >$; this quantity goes from $\frac{1}{8}n(2-n)$ for $U = 0$ to zero for $U \to \infty$.

As can be seen in the figure, spin excitations always have a gap at least of the order of 2Δ, because creating this type of excitation necessarily implies breaking a pair. In the case of small U, finite-size effects are strong and the spin gap is larger than expected for the thermodynamic limit. In the mean-field approach, the spin excitation corresponds to creating two BCS quasiparticles with the same spin. In the small cluster, and due to the Pauli principle, the lowest excited state contains one BCS quasiparticle with an energy equal to the one-particle gap and another with a different $\mathbf{k}$ and a significantly larger energy.

In Fig. 11 the spectral density of spin excitations $-(1/\pi)\mathrm{Im}\chi(\mathbf{q},\omega)$ is shown for all values of $\mathbf{q}$. If we calculate the spin-excitation energies as a sum of two BCS quasiparticle energies, the lowest state for almost every $\mathbf{q}$ is well reproduced in weak coupling (see solid line in the figure). As U increases, the lowest energy is below the mean-field result. This is related to the residual interaction between BCS quasiparticles that renormalize the mean-field results.

E. Quasiparticles

As we mentioned above, there are one-particle excitations with energies much smaller than the mean-field energy $E_{\mathbf{k}}$. In the one-particle spectral density $A(\mathbf{k},\omega)$, the peak with energy nearest to the chemical potential corresponds to a real quasiparticle state. The quasiparticle peak has a dispersion relation with a bandwidth that is strongly reduced as U increases. These quasiparticle states can be viewed as Bogoliubov quasiparticles that are strongly dressed by collective excitations. The collective excitations that will renormalize the one-particle excitations are the charge and spin excitations discussed above. However, as we showed, in the intermediate or large-U limits, charge and spin excitations have different characteristic energy scales, the former being low-energy excitations and the latter having energies larger than 2Δ.

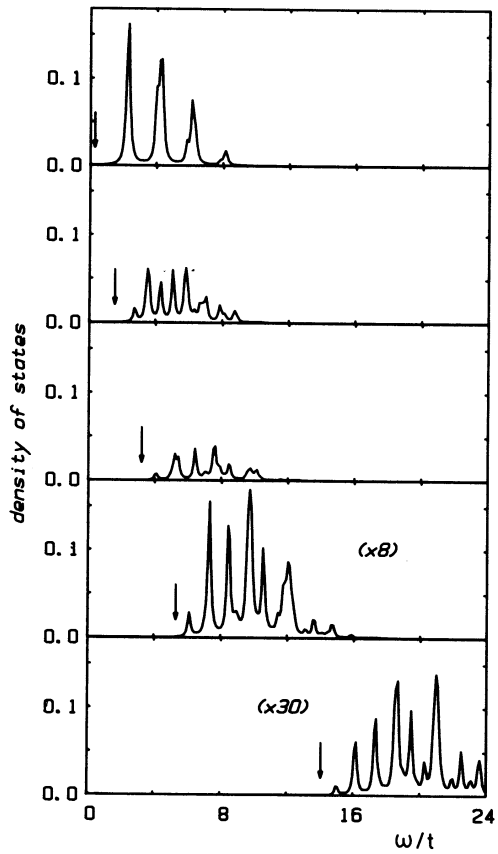

FIG. 10. Total density of spin excitations for $N_e = 4$, with $U = 1, 4, 7, 10$, and 20 (from upper to lower boxes); and $\eta = 0.1t$. For $U = 10$ and 20 the spectral weight was multiplied by the factors indicated in the figure in order to make it visible in the plot. The arrows show the position of 2Δ for each value of U.

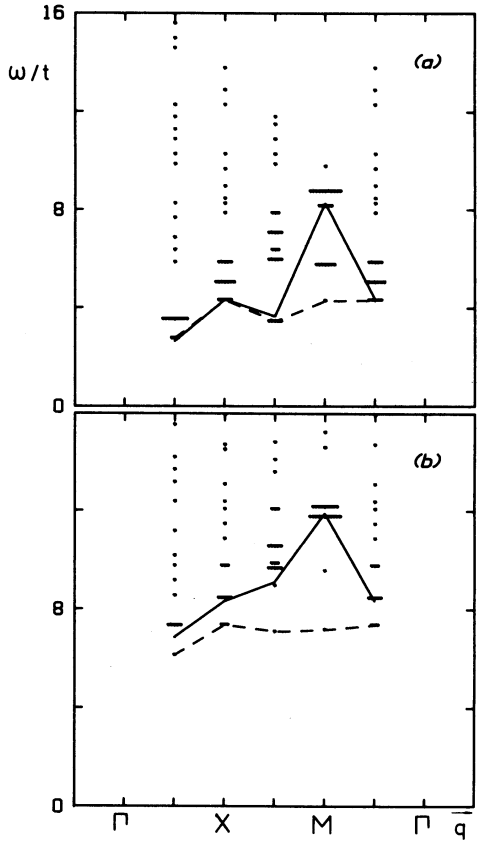

FIG. 11. Spectral densities of spin excitations for $N_e = 4$ and all values of $\mathbf{q}$ with (a) $U = 4$ and (b) $U = 10$. The plot is done as in Fig. 7. Dashed and solid lines are guides to the eye, the former join the lowest exact spin-excitation energies, the later join the lowest spin-excitation energies in the BCS approximation (see text).

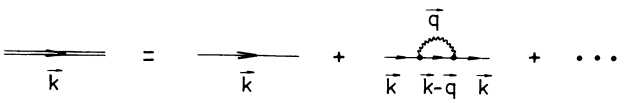

FIG. 12. Perturbative corrections to the BCS quasiparticle. The wiggled line represents a collective excitation.

In this situation we expect the charge excitations to be the most important in dressing the one-particle excitations. The one-particle propagator has corrections which are schematically shown in Fig. 12. In the lowest order, the energy of this one-particle excitation is given by the minimum energy of all the states that contribute to its wave function. In particular, for $\mathbf{k}$ away from k_F, this energy is $E_{k_F} + \omega_{\mathbf{k}-\mathbf{k}_F}$, where $\omega_{\mathbf{q}}$ is the energy of a collective excitation of momentum $\mathbf{q}$. Since the charge excitations have a narrow bandwidth for large U, this energy is much smaller than $E_{\mathbf{k}}$. We calculate the energy of the quasiparticle peak using this criterion and compare with the exact results. In Fig. 13 both dispersion relations

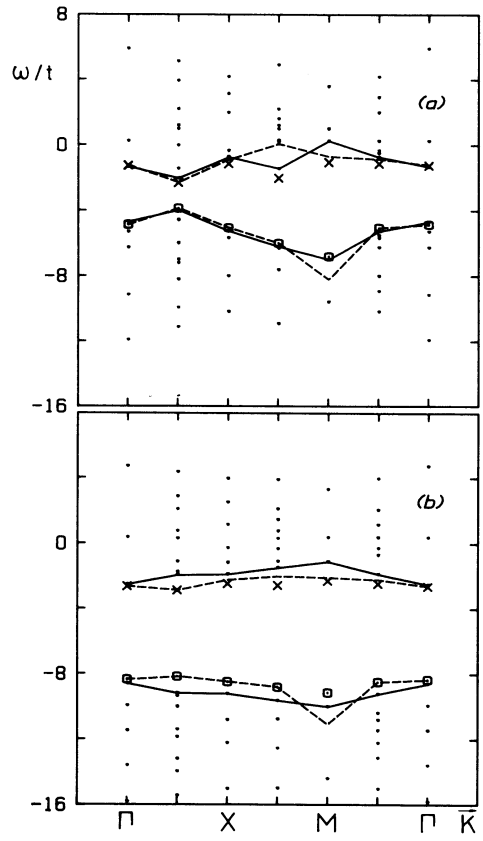

FIG. 13. Quasiparticle energies vs $\mathbf{k}$ for $N_e = 4$ with (a) $U = 4$ and (b) $U = 10$. Points: spectra obtained with the zero-order approximation discussed in the text, (×) energy differences between the exact ground state with $N_e + 1$ particles in each symmetry subspace and the ground state with N_e particles, (□) energy differences between the ground state with N_e particles and the ground state with $N_e - 1$ particles in each symmetry subspace. Dashed and solid lines are guides to the eye, the former joins the exact quasiparticle energies obtained from the one-particle spectral densities, the latter joins the minima of the zero-order spectra.

are shown. For small U, the agreement is quantitative, except that some states appear that have zero weight in the exact calculation.

As U increases some small differences can be observed. This can be understood in terms of the mixing between different states in Fig. 12, the mixing matrix elements being larger for large U. This is consistent with the fact that exact quasiparticle energies are generally lower than the approximate energies obtained by the zero order minimum energy criterion.

As we mentioned above, and is shown in the figure, there are some states that do not appear in the exact one-particle spectrum. We have checked that there are states with $N_e + 1$ or $N_e - 1$ particles with energies very close to the ones predicted by our simple criterion (see Fig. 13). These states are not observed in the exact spectral densities because the matrix element of $c^\dagger_{\mathbf{k}\sigma}$ ($c_{\mathbf{k}\sigma}$) connecting the ground state with N_e particles to the ground state with $N_e + 1$ ($N_e - 1$) particles and momentum $\mathbf{k}$ ($-\mathbf{k}$) is lower than the error in the numerical calculation of the wave functions (10^{-8}). It could be possible that these matrix elements were exactly zero because of a selection rule based on a symmetry operation; however, it was checked that the transformation properties of the initial and final states in each case were compatible with a nonzero value for the matrix element.

To sum up, we have presented clear evidence that the low-energy one-particle excitations are strongly dressed Bogoliubov quasiparticles. These dressed quasiparticles have been studied in the large-U limit by mapping the problem into the polarized t-J model[8,9] and are related to the pairing bag excitations discussed by Bishop *et al.* using a mean-field Bogoliubov–de Gennes approach.[15]

IV. SUMMARY AND DISCUSSION

In this work we studied the negative-U Hubbard model by exact diagonalization methods in a 4 × 4 cluster, we obtained results for different values of U and particle densities. Our results concern ground-state properties on one hand and elementary excitations on the other and can be summarized as follows.

For the ground state we showed the following.

(a) The BCS approximation gives very good results for the energy and wave function for the whole range of values of U. The largest discrepancies appear for $U \simeq W = 4t$, but even in this case the BCS energy is correct within 3.5% or less. The expectation values $\langle c^\dagger_{\mathbf{k}\sigma} c_{\mathbf{k}\sigma} \rangle$ calculated in the ground state deviates slightly from the BCS result only for $\mathbf{k} = 0$ and $U \simeq W$.

(b) The chemical potential is also in good agreement with the BCS estimate, it increases as the density increases and may get into the Hartree-Fock band.

For the elementary excitations our results are the following.

(c) The total one-particle density of states shows a gap pinned to the Fermi energy. Again the gap is well reproduced in the BCS approximation.

(d) Charge excitations of two kinds are observed: pair-breaking excitations with energy larger than 2Δ and collective excitations with lower energy. For intermediate to

large U the two types of excitations are well separated in energy, and collective excitations carry most of the spectral weight. For small U, however, the two types of excitations are not so clearly separated and pair-breaking excitations have large spectral weight. The results for the energy of the collective mode are qualitatively well reproduced in the RPA approximation.

(e) Spin excitations always have a gap at least of the order of 2Δ, because creating this type for excitation necessarily involves breaking a pair. The total weight of spin excitations is proportional to the square of the magnetic moment, and goes to zero for $U \rightarrow \infty$ as the magnetic moment is suppressed by the interaction.

(f) The one-particle spectral densities show two especially interesting features. On one hand, the BCS dispersion relation almost fits the position of the most intense peaks of the exact calculation. We argue that these intense peaks will give rise in the thermodynamic limit to a resonance with a finite width. On the other hand, the quasiparticle peaks, which for most values of $\mathbf{k}$ have a lower intensity, have a dispersion relation with a larger effective mass. This can be understood as a result of strong dressing of the Bogoliubov quasiparticles by collective charge excitations. These quasiparticles can be associated with the pairing bags discussed in Refs. 15 and 8. An open issue is what would happen with the quasiparticle dispersion relation in a more realistic model where the long-range Coulomb repulsion changed low-energy charge excitations for $q \rightarrow 0$ into high-energy plasma modes.

---

*Permanent address: Departamento de Física, CNEA, Avenida del Libertador 8250, 1429 Buenos Aires, Argentina.

[1] M. Randeria, J. Duan, and L. Shieh, Phys. Rev. B **41**, 327 (1990).

[2] R. T. Scalettar, E. Loh, J. Gubernatis, A. Moreo, S. White, D. Scalapino, R. Sugar, and E. Dagotto , Phys. Rev. Lett. **62**, 1407 (1989).

[3] J. O. Sofo, C. A. Balseiro, and H. E. Castillo, Phys. Rev. B (to be published).

[4] A. J. Leggett, in *Modern Trends in the Theory of Condensed Matter*, edited by A. Pekalski and J. Przystawa (Springer-Verlag, Berlin, 1980), p. 13.

[5] P. Nozières and S. Schmitt-Rink, J. Low Temp. Phys. **59**, 195 (1985).

[6] J. O. Sofo and C. A. Balseiro (unpublished).

[7] E. R. Gagliano *et al.*, Phys. Rev. B **34**, 1677 (1986); E. R. Gagliano and C. A. Balseiro, Phys. Rev. Lett. **59**, 2999 (1987); R. Haidock, V. Heine, and M. Kelly, J. Phys. C **5**, 2845 (1972).

[8] A. G. Rojo, J. O. Sofo, and C. A. Balseiro, Phys. Rev. B **42**, 10 241 (1990).

[9] K. Hallberg, A. G. Rojo, and C. A. Balseiro, Phys. Rev. B **43**, 8005 (1991).

[10] See, for example, R. Micnas, J. Ranninger, and S. Robaszkiewicz, Rev. Mod. Phys. **62**, 113 (1990); and references therein.

[11] E. Dagotto *et al.* (unpublished).

[12] S. Robaszkiewicz, R. Micnas, and K. A. Chao, Phys. Rev. B **23**, 1447 (1981).

[13] A. Alexandrov and J. Ranninger, Phys. Rev. B **23**, 1796 (1981).

[14] S. C. Zhang, Phys. Rev. Lett. **65**, 120 (1990).

[15] A. R. Bishop, P. S. Lomdahl, J. R. Schrieffer, and S. A. Trugman, Phys. Rev. Lett. **61**, 2709 (1988).